Chirality reversal of the interface domain wall in a hard/soft magnetic bilayer

Y. Henry, S. Mangin, F. Montaigne

PHYSICAL REVIEW B **69**, 140401(R) (2004)

Chirality reversal of the interface domain wall in a hard/soft magnetic bilayer

Y. Henry*
Institut de Physique et Chimie des Matériaux de Strasbourg, CNRS and Université Louis Pasteur, Boîte Postale 43, F-67034 Strasbourg Cedex 2, France

S. Mangin and F. Montaigne
Laboratoire de Physique des Matériaux, Université H. Poincaré, Boîte Postale 239, F-54506 Vandoeuvre-les-Nancy Cedex, France
(Received 10 February 2004; published 2 April 2004)

The change of chirality of the interface domain wall formed in a hard/soft exchange-coupled bilayer submitted to an in-plane rotating field is studied experimentally through the anisotropic magnetoresistance response of the film. It is shown that the chirality reversal can take place in one or two stages, depending on the field strength. The irreversible transitions which occur during the two-stage process correspond to an unwinding and a rewinding in the opposite sense of the magnetic profile. The formation of multidomain structures during these transitions is evidenced and shown to be of prime importance for the understanding of the reversal process.

DOI: 10.1103/PhysRevB.69.140401 PACS number(s): 75.60.Ch, 75.30.Et, 75.70.Cn

Thin-film exchange-spring magnets made of the juxtaposition of hard and soft ferromagnetic (or ferrimagnetic) layers constitute model systems as they offer the ability to create and study well-controlled artificial Bloch-like walls of simple geometry.[1] In the past, many works have been devoted to the determination of the magnetic profiles which form in such structures upon reversal of the applied magnetic field.[1–10] Much fewer have been dedicated to the understanding of what happens upon rotation of the field.[11,12] In this case, experimental evidences have been given recently that a laterally uniform interface domain wall (iDW) may form and undergo an abrupt change of chirality, at a certain critical angle. Micromagnetic models developed to predict the value of this angle have failed to reproduce experimental data so that the process by which the chirality reversal actually occurs remains essentially unknown. It is the purpose of the present work to bring insights into this unusual reversal process.

In a previous paper,[12] we studied theoretically how a hard/soft bilayer is expected to behave in a rotating magnetic field as a function of the field amplitude and soft layer thickness. In the model used, the hard layer magnetization was assumed perfectly rigid and the soft layer was treated as a one-dimensional chain of spins with in-plane uniaxial anisotropy, running normal to the interface.[13] The anisotropic magnetoresistance (AMR) associated with the stable magnetic configurations of the bilayer was determined and compared successfully with experimental data taken on a $Tb_{55}Fe_{45}(50\ nm)/Gd_{40}Fe_{60}(100\ nm)$ ferrimagnetic stack. The manifold of qualitatively different field regimes predicted by our model for this particular sample was observed experimentally. This proved the ability of our theoretical approach to determine the stable magnetic configurations in such a system.

In the present work, we focus on a similar amorphous $Tb_{55}Fe_{45}(50\ nm)/Gd_{40}Fe_{60}(t)$ hard/soft ferrimagnetic bilayer, but with a thinner soft GdFe layer ($t=50$ nm). In this case, the iDW extends over a larger fraction of the sample. As a result, the chirality change gives rise to a larger variation of AMR, which makes its study somewhat easier. As in the sample studied in Ref. 12, the soft layer exhibits a well-defined uniaxial anisotropy in the plane. Here, the GdFe anisotropy field amounts to $H_a=(211\pm5)$ Oe at 20 K. Electrical resistivity measurements on this sample were carried out at 20 K, using a conventional four-wire method. These were performed in the usual current-in-plane geometry after the sample had been cooled down from room temperature in a field of 10 kOe applied along the current direction $\hat{\mathbf{i}}$. This direction was within a couple of degrees from the easy axis of magnetization of the GdFe layer $\hat{\mathbf{u}}$. The field cooling induces in TbFe a very high remanent magnetization which is strongly constrained along the cooling-field direction,[14] hence along $\hat{\mathbf{i}}$. At 20 K, TbFe is then extremely hard magnetically (switching field of the order of 10 kOe) and its magnetization remains essentially unaffected by the application of fields of several hundreds of oersteds. After stabilization of the sample temperature to better than 0.05 K,[15] and reduction of the external field amplitude to the required value, the sample resistance R was monitored while the field $\mathbf{H}$ of angle ψ (as measured from $\hat{\mathbf{i}}$) was rotated in the plane of the film, with a constant angular velocity of 0.5°/s. Data were taken successively for counterclockwise (CCW) and clockwise (CW) directions of rotation. This entire procedure ensured that, at the beginning of each experiment, the hard and soft layers could be considered as uniformly magnetized along $\hat{\mathbf{i}}\sim\hat{\mathbf{u}}$, a situation which corresponds to the largest possible resistance of the bilayer ($R_{\parallel}$).

Figure 1 shows examples of AMR curves recorded in the so-called low-field regime [Fig. 1(c)] and high-field regime [Fig. 1(f)]. Also shown are the corresponding theoretical curves computed using the model of Ref. 12. These data illustrate the differences which exist between the two regimes. For low applied fields, there is a single stable magnetic configuration accessible, σ_0, whatever be the orientation of the field. The magnetization profile always evolves in a reversible manner with varying ψ. No large twist of the magnetization distribution develops in the soft layer. In the

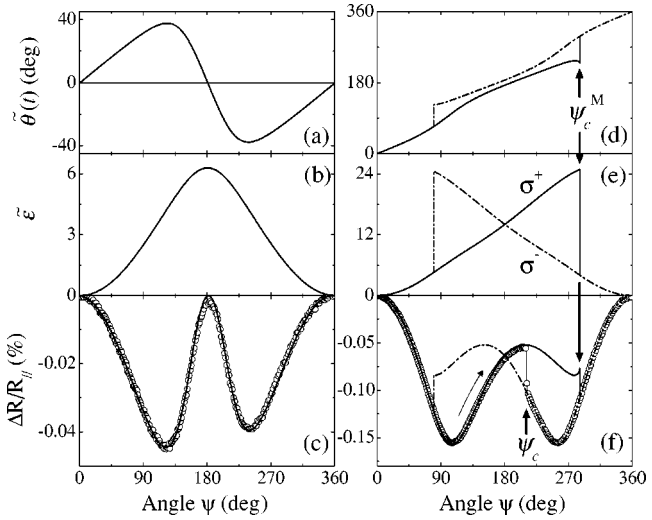

FIG. 1. (c,f) Counterclockwise AMR curves $\Delta R/R_{\|}=[R(\psi)-R_{\|}]/R_{\|}$ (where $R_{\|}=37.1792\ \Omega$) deduced from experiment (○) and computed (lines), for two field values, (c) 150 Oe, and (f) 600 Oe, belonging to the low-field regime and high-field regime, respectively. Also shown are the corresponding theoretical angular variations of the angle $\tilde{\theta}(t)$ (a,d) and of the total energy $\tilde{\epsilon}$ (b,e) associated with the stable magnetic profile(s) of the soft layer. Solid and dashed lines in (d–f) correspond to the σ^+ and σ^- profiles, respectively. For the simulations, we assumed an angle of 1° between the current direction and the soft layer easy axis, an exchange length $\lambda=22$ nm (after Ref. 12), and $H_a=211$ Oe.

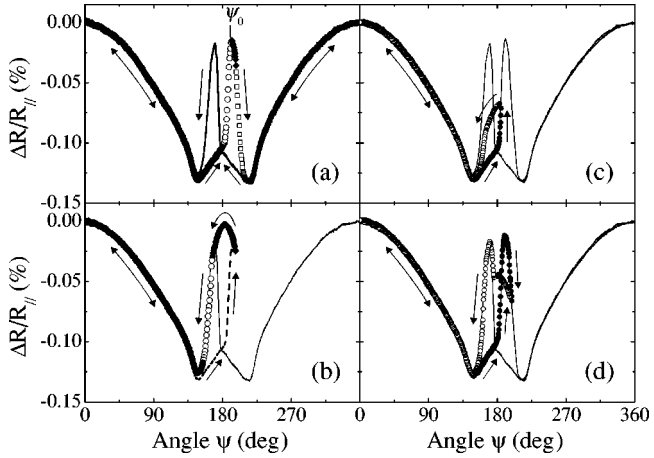

FIG. 2. AMR curves measured with a rotating field of 198 Oe ($H/H_a=0.94$). (a) Major counterclockwise (symbols) and clockwise (line) curves. Solid (open) symbols indicate the reversible (irreversible) parts of the CCW curve. (b) Minor AMR curves recorded by first rotating the field counterclockwise (dashed line) up to $\psi_R=197°$, then clockwise (symbols) down to $\psi=0°$. (c,d) Minor curves (symbols) recorded following the same procedure as in (b) with $\psi_R=185°$ (c) and $\psi_R=200°$ (d). The solid lines in (b,c,d) are the major curves shown in (a).

case depicted in Figs. 1(a)–1(c) ($H/H_a=0.71$), the angle $\tilde{\theta}(t)$ of the last spin of the chain (furthest from the hard layer) never exceeds 40°. In the high-field regime, on the contrary, two possible magnetization profiles exist for certain field orientations and irreversible transitions from one configuration to another occur, which correspond to an inversion of the chirality of the iDW, as we shall discuss now. In the case shown in Figs. 1(d)–1(f) ($H/H_a=2.84$), the configuration σ^+ initially adopted by the system as the field is rotated CCW away from the pinning (current) direction is a Bloch-like wall in which the spins rotate CCW with increasing distance from the hard layer. It becomes metastable as ψ exceeds $\psi_c^m=180°$ [Fig. 1(e)]. Beyond ψ_c^m, it would be energetically advantageous for the system to switch into another magnetic configuration σ^- corresponding to a profile of opposite chirality, i.e., in which the spins rotate CW. However, an energy barrier separates the two states. According to our model, the latter disappears only as ψ passes ψ_c^M ($\psi_c^M=286°$ for $H/H_a=2.84$) and the chirality reversal occurs by unwinding of the wall.[12] Experimentally [Fig. 1(f)], the iDW is found to reverse its chirality at an intermediate angle ψ_c (211° for $H/H_a=2.84$), between ψ_c^m and ψ_c^M. Although experimental and calculated data agree extremely well as far as the stable configurations are concerned [Fig. 1(f)], the lack of agreement about the chirality reversal angle and the absence of experimental indications of the wall unwinding do not allow us to conclude, from an experiment such as that of Fig. 1(f), on how the magnetization really behaves during the reversal process.

Most interestingly, our model predicts the existence of an intermediary-field regime in which three stable magnetic configurations may coexist. The first two of them are of the types described just before: the σ^+ and σ^- configurations corresponding to profiles of possibly large twists and opposite chiralities. The third one is equivalent to the only stable configuration accessible in the low-field regime, σ_0, yet with the major difference that it exists only in a restricted angle range, around $\psi=180°$. It corresponds to a profile in which *all* the spins are roughly aligned antiparallel to the field. In these conditions, a two-stage chirality reversal is susceptible to occur, in which the magnetization would adopt successively the σ^+, σ^0, and σ^- configurations upon rotation of the external field in the CCW direction.

Experimental evidence of such a two-stage process is given in Fig. 2(a). Let us analyze in detail the AMR curve taken for the CCW direction of rotation [symbols in Fig. 2(a)]. The first part of this curve (●), running from $\psi=0°$ to $\psi=180°$, is similar in shape to the one measured in higher field [Fig. 1(f)]. It corresponds to the progressive winding of a σ^+ profile of large twist [compare $R(180°)$ and $R(0°)$]. As ψ exceeds 180°, the resistance increases sharply (○) to reach a level close to the maximum resistance $R_{\|}$. This high resistance is necessarily associated with a configuration in which *all* the spins are oriented close to the current direction. Since a rotation of a majority of the spins towards the 180° direction can be excluded on obvious physical grounds, the sharp increase observed can undoubtedly be attributed to an abrupt unwinding of the profile, i.e., to a $\sigma^+\rightarrow\sigma^0$ transition. Beyond the angle $\psi^0=191°$ where it reaches a maximum, the resistance first decreases slowly with increasing angle (◆). The system remains in the σ^0 configuration, while the (small) magnetization twist slightly increases. Then the resistance decreases abruptly (□). This corresponds to the

sudden reformation of a magnetic profile of large twist. We note that the subsequent variation of resistance (■) follows the very same AMR curve as the one measured before any transition when rotating the field CW [line in Fig. 2(a)], that is, upon formation of a σ^- profile. Then, on the basis of trivial symmetry arguments, we can state that (i) the second abrupt change in resistance reveals a $\sigma^0 \rightarrow \sigma^-$ transition, i.e., a rapid winding of the spins in the opposite (CW) direction, and that (ii) this transition is eventually followed by a slow unwinding of the σ^- profile as-formed.

In order to further demonstrate that the intermediate configuration σ^0 temporarily adopted by the system during the chirality reversal process is indeed a configuration analogous to that occurring in the low-field regime, we also carried out an experiment in which the rotation of the field (CCW) was stopped after the sample had been brought to the σ^0 state, and then resumed in the opposite (CW) direction, while the sample resistance was constantly monitored. The minor AMR curve obtained in this way is presented in Fig. 2(b). One should first notice that, after the direction of rotation was reversed, and ψ decreased below ψ^0, the resistance (symbols) does not show the same angular variation as before (dashed line). This is a clear evidence of the irreversibility of the $\sigma^+ \rightarrow \sigma^0$ transition. Second, the AMR curve taken after the change of direction may be decomposed in two parts. The first one (♦) has a bell shape and closely obeys $R(180^o)=R(0^o)$, as well as the symmetry relationship $R(180^o-\psi)=R(180^o+\psi)$, three characteristic features of the AMR curves obtained in the low field regime [Fig. 1(c)], hence of a profile of type σ^0. The second part (circles) superposes on the major CW curve (solid line). Using symmetry arguments once more, it can be ascertained that it corresponds to a $\sigma^0 \rightarrow \sigma^+$ transition (○) and the subsequent unwinding of the σ^+ profile (●).

The scenario proposed which describes the chirality reversal as a two-stage process was elaborated on the basis of purely empirical arguments. Hereafter, we shall show that it is also supported by one-dimensional model calculations. Experimentally, the transitions are found to have an angular width of several degrees [Fig. 2(a)]. In most of the discussion that follows, we will however ignore this aspect and define the angular position of the transitions precisely at the location of the largest experimental gradient $dR/d\psi$, considered as representative of the ''average'' sample. Figure 3(b) shows that the theoretical AMR curves reproduce the experimental data of Fig. 2(a) extremely well. This proves once again the ability of our model to determine the magnetic configurations adopted by the TbFe/GdFe bilayer. From the comparison between measured and calculated AMR data it is now possible to identify for sure in what magnetic state the bilayer system actually finds itself (symbols in Fig. 3) for any ψ (except those angles where the transitions occur). By doing this, one readily confirms that, upon rotation of the external field from 0 to 360°, the system occupies successively the σ^+, σ^0, and σ^- states.

Figures 3(c) and 3(d) show the energy of the σ^+, σ^0, and σ^- configurations [Fig. 3(c)] and the height of the intrinsic energy barriers between them [Fig. 3(d)], as a function of ψ, in the angular range where the $\sigma^+ \rightarrow \sigma^0$ ($\psi=187^o$) and $\sigma^0 \rightarrow \sigma^-$ ($\psi=200^o$) transitions are detected experimentally. These theoretical data obtained considering a laterally invariant magnetization distribution are not able to account for all aspects of the experimental observations. On the contrary, we may point out two contradictions or inconsistencies between experimental and theoretical results. First, a close inspection of Fig. 3(c) allows one to see that, while the barrier heights are identical for the two transitions ($\Delta\epsilon_+^- = \Delta\epsilon_+^0$), the gain in energy would be (slightly) larger if the system switched from σ^+ to σ^-, rather than to σ^0. Therefore a direct one-stage $\sigma^+ \rightarrow \sigma^-$ reversal should be favored. Second, Fig. 3(d) shows that, during the $\sigma^+ \rightarrow \sigma^0$ transition, the system is able to overcome a large energy barrier, whereas for the $\sigma^0 \rightarrow \sigma^-$ transition it cannot do so and the corresponding barrier has to vanish before the transition can take place. In the sequel, we shall show that these inconsistencies, which reveal the limits of validity of our model, disappear when one considers the formation of multidomain structures during the transitions.

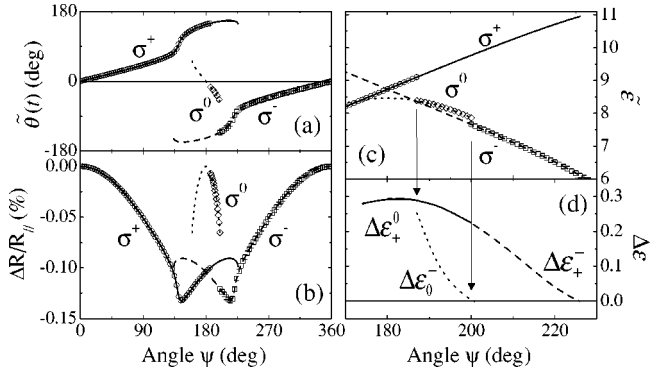

FIG. 3. Results of the model calculations for $t/\lambda=2.25$ and $H/H_a=0.94$. (a) Angle of the last spin $\tilde{\theta}(t)$, (b) magnetoresistance ratio, (c) magnetic energy of the soft layer $\tilde{\epsilon}$, and (d) height of some intrinsic energy barriers, as a function of the field angle ψ. The solid, dashed, and dotted lines in (a,b,c) correspond to magnetic profiles of the type σ^+, σ^-, and σ^0, respectively. The symbols indicate the states effectively occupied by the TbFe/GdFe bilayer, as deduced from the comparison of computed and experimental AMR data (see text for details). The solid, dashed, and dotted lines in (d) correspond to the energy barriers between the σ^+ and σ^0 states ($\Delta\epsilon_+^0$), the σ^+ and σ^- states ($\Delta\epsilon_+^-$), and the σ^0 and σ^- states ($\Delta\epsilon_0^-$), respectively.

Figures 2(c) and 2(d) show the results of experiments where the direction of rotation of the field was reversed from CCW to CW while the system was switching from σ^+ to σ^0 [Fig. 2(c)] and from σ^0 to σ^- [Fig. 2(d)]. It is clear from these measurements that the sample contained both switched and nonswitched domains and then that the transitions occur indeed in a laterally nonuniform manner, through the nucleation of ''reversed domains.'' Such nuclei must necessarily be separated from the surrounding nonswitched phase by some kind of complex lateral domain walls (LDW's), in which the magnetization direction varies not only with the perpendicular-to-plane coordinate, as in domains of σ^+ or σ^- configuration, but also with the in-plane coordinates. Of course, the creation of a LDW has a certain energy cost. As

in the usual case of the magnetization reversal, it is only if the energy gain generated by the change of magnetic configuration inside the domain exceeds the wall cost that a switched domain can be created. Having pointed out that, the inconsistencies mentioned above can now be resolved by considering the gain-versus-cost balance in each case.

What differentiates mostly the $\sigma^+ \rightarrow \sigma^-$ transition from the $\sigma^+ \rightarrow \sigma^0$ one is not the energy gain but the wall cost. Indeed, because of their necessarily larger degree of magnetization rotation, LDW's separating domains of σ^+ and σ^- configurations must have an energy much larger than LDW's between regions of σ^+ and σ^0 configurations. In these conditions, the direct $\sigma^+ \rightarrow \sigma^-$ transition might well be hindered because of the prohibitive energy of the walls involved, leaving the $\sigma^+ \rightarrow \sigma^0$ transition as the only one allowed. In contrast, the $\sigma^+ \rightarrow \sigma^0$ and $\sigma^0 \rightarrow \sigma^-$ transitions do not differ strongly in the wall cost. Indeed, for symmetry reasons, the energy of the two types of LDW involved (σ^0/σ^+ and σ^0/σ^-) must be quite similar, as long as $\psi \sim 180^o$. These transitions rather differ in the energy gain [see Fig. 3(c)]. The one associated with the $\sigma^+ \rightarrow \sigma^0$ transition rises rapidly with increasing ψ. This makes the nucleation of σ^0 domains possible relatively quickly after σ^+ has become metastable, and well before it becomes unstable ($\psi > 226^o$). Comparatively, the gain of the $\sigma^0 \rightarrow \sigma^-$ transition remains small and almost constant with varying ψ. A gain too low in comparison with the wall cost is certainly the reason why the $\sigma^0 \rightarrow \sigma^-$ transition occurs only when σ^0 stops being (meta)stable and the system is forced to fall into the ground-state σ^- ($\psi = 200^o$).

To end this discussion, we wish to draw attention to the fact that the transitions detected upon rotation of the magnetic field CW, when starting from a multidomain state, either (σ^+, σ^0) [Fig. 2(c)] or (σ^0, σ^-) [Fig. 2(d)], occur almost at the same angles as in the case where the sample is initially in a single-configuration state (major AMR curves). This implies that lateral domain expansion (LDW propagation) is limited and suggests that the reversal mechanism is dominated by nucleation. Then, the finite angular width of the transitions arises probably from a distribution of nucleation angle, due to lateral inhomogeneities in the sample (e.g., local variations of thickness or magnetic anisotropy).

In summary, we have brought clear evidence that, in a hard/soft exchange-coupled bilayer submitted to a rotating in-plane magnetic field, the twisted magnetization profile formed at the interface may change its chirality in one or two stages, depending on the field amplitude. The irreversible transitions which take place during the two-stage process correspond, respectively, to an unwinding and a rewinding of the spins in the opposite sense. They occur essentially by nucleation of switched domains.

*Electronic address: Yves.Henry@ipcms.u-strasbg.fr

[1] K. Mibu, T. Nagahama, and T. Shinjo, J. Magn. Magn. Mater. **163**, 75 (1996).

[2] K. Mibu, T. Nagahama, T. Shinjo, and T. Ono, Phys. Rev. B **58**, 6442 (1998).

[3] T. Nagahama, K. Mibu, and T. Shinjo, J. Phys. D **31**, 43 (1998).

[4] E.E. Fullerton, J.S. Jiang, M. Grimsditch, C.H. Sowers, and S.D. Bader, Phys. Rev. B **58**, 12 193 (1998).

[5] E.E. Fullerton, J.S. Jiang, and S.D. Bader, J. Magn. Magn. Mater. **200**, 392 (1999).

[6] S. Mangin, C. Bellouard, and H. Fritzsche, Physica B **276-278**, 558 (2000).

[7] O. Hellwig, J.B. Kortright, K. Takano, and E.E. Fullerton, Phys. Rev. B **62**, 11 694 (2000).

[8] K.V. O'Donovan, J.A. Borchers, C.F. Majkrzak, O. Hellwig, and E.E. Fullerton, Phys. Rev. Lett. **88**, 067201 (2002).

[9] R. Röhlsberger, H. Thomas, K. Schlage, E. Burkel, O. Leupold, and R. Rüffer, Phys. Rev. Lett. **89**, 237201 (2002).

[10] V.E. Kuncser, M. Doi, W. Keune, M. Askin, H. Spies, J.S. Jiang, A. Inomata, and S.D. Bader, Phys. Rev. B **68**, 064416 (2003).

[11] C.L. Platt, A.E. Berkowitz, S. David, E.E. Fullerton, J.S. Jiang, and S.D. Bader, Appl. Phys. Lett. **79**, 3992 (2001).

[12] F. Montaigne, S. Mangin, and Y. Henry, Phys. Rev. B **67**, 144412 (2003).

[13] In this model, the behavior of the bilayer is entirely determined by two *fixed* parameters only: the ratio of the thickness t to the exchange length λ of the soft layer and the ratio of the applied magnetic field H to the soft layer anisotropy field H_a.

[14] S. Mangin, G. Marchal, and B. Barbara, Phys. Rev. Lett. **82**, 4336 (1999).

[15] Good stabilization of the sample temperature was necessary since the AMR of $Gd_{40}Fe_{60}$ is only $(\rho_\parallel - \rho_\perp)/\rho_\parallel = 0.3\%$ ($\rho_\parallel = 310\ \mu\Omega$ cm), while its temperature coefficient of resistivity $1/\rho_\parallel \times d\rho_\parallel/dT$ amounts to -270 ppm/K, in the temperature range around 20 K.